Dynamic Response Criteria for a Large Child ATD Thoracic Spine

Jason A. Stammen[1], Bruce R. Donnelly[1], Brian Suntay[2], Kevin M. Moorhouse[1]

Abstract The large omnidirectional child (LODC) anthropomorphic test device (ATD) thorax has a flexible thoracic spine to address chin-to-chest contacts in existing child ATDs. To compare this 10 year old-sized ATD response to human spine data, a biofidelity target was derived by scaling and normalizing adult post-mortem human subject (PMHS) thoracic spine dynamic responses to a characteristic 10 year old human response. LODC thoracic spine biofidelity was then evaluated in the same experimental configurations as in previously conducted adult PMHS tests (Isolated Segment Manipulation (ISM), 3.8 and 5.0 m/s frontal sled with vertebral fixation). The LODC demonstrated a thoracic spine response and head kinematic characteristics that approximated scaled human data. The effective stiffness of the LODC in the ISM condition displayed a similar ratio with respect to the adult stiffness as the stiffness scale factor using a published scaling technique. The LODC spine is stiffer than estimated large child human spine response targets and displayed a bi-modal response characteristic that differed from the uni-modal human response shape. This behavior was attributed to low cervicothoracic rotational stiffness given very little cervical (neck) flexion. The LODC response was repeatable until spine degradation was discovered near the end of the 5.0 m/s sled series. While the LODC thoracic spine requires more refinement to more closely approximate human response, it shows promise as an enhancement to existing rigid ATD spine designs.

Keywords anthropomorphic test device, biomechanics, dynamic response, pediatric, thoracic spine

I. INTRODUCTION

Child anthropomorphic test devices (ATDs) have been shown to have greater head rotational velocities and lower head excursions than real or estimated human responses [1-6], and this behavior can result in hard chin to chest contacts in certain restraint situations [7-8]. These characteristics have been attributed primarily to a rigid thoracic spine structure in the ATD. While the effectiveness of belt-positioning booster (BPB) seats is well known [9], chin to chest contacts observed in the Hybrid III ten year old dummy has excluded the use of HIC for evaluating head protection in FMVSS No. 213 child restraint tests.

While there is a lack of high-speed pediatric data, many studies have identified distinct structural differences in the spine with age. Developmental differences have been observed in cervical spine mechanical properties [10-12], spinal ligament composition [13], and vertebral level of spinal injuries [14]. Weaker musculature, a larger relative head mass, and less spinal curvature have also been correlated to age differences in range of motion [15-17]. The combined effect of these developmental differences suggests significantly more spine flexibility in children than in adults. These studies have focused primarily on the cervical spine; the identification of thoracic spine dynamics has been a challenge due to the complex integration within the thorax [18].

A review of the literature shows that only 11 pediatric post-mortem human subjects (PMHS) have been tested in vehicle restraint conditions [19-24]. Because of ethical concerns about high speed evaluations of pediatric specimen response, child ATD targets are typically developed using scaling techniques. Scaling methodologies using some combination of mass, length, and stiffness factors have historically been used to develop child ATD load vs. displacement criteria for the head, neck, and thorax [25-26]. However, no such response target has been derived for the thoracic spine of child ATDs. A recent study by Arbogast et al. [27] examined spine kinematics from adult and child volunteers in the same low speed test condition. This study showed distinctive differences in spinal displacement and rotation with age. This data was subsequently used by Lopez-Valdes et al. [28] with both

[1]J.A. Stammen, Ph.D. (tel: +937-666-3319, fax: +937-666-3590, jason.stammen@dot.gov), B.R. Donnelly, Ph.D., K. M. Moorhouse, Ph.D., National Highway Traffic Safety Administration, Vehicle Research & Test Center, U.S. Department of Transportation, Washington, DC.
[2]B. Suntay, Transportation Research Center Inc., East Liberty, OH.

low and high speed adult PMHS data to derive an energy-based scaling approach utilizing relative mass, belt tension, and trajectory/path lengths in an effort to predict high speed pediatric (6 year old) kinematics. While this approach improved upon the kinematic predictions provided by earlier scaling methods, experimental displacements were under-predicted.

To address concerns with head kinematics and neck loads, a force vs. displacement target for the upper thoracic spine would provide a guideline for ATD design. Thoracic spine dynamic data from adult PMHS was obtained by Stammen et al. [29-30] through novel experimental approaches in both bench-top (Isolated Segment Manipulation) and coupled mid-spine sled test conditions. The objectives of this study are to (1) apply published scaling and normalization techniques to this adult PMHS data to obtain a large child ATD target; (2) test a new prototype large omnidirectional child (LODC) ATD in the same conditions as the adult PMHS; and (3) compare the LODC thoracic spine response to the PMHS-based large child target.

II. METHODS

Four steps were taken in this study to evaluate the LODC thoracic spine response: (1) scale adult PMHS data to an estimated large (10 year old) child using published methods, (2) normalize the scaled data to obtain a characteristic response target, (3) test the LODC in the same biofidelity experiments as the adult PMHS, and (4) quantitatively compare the LODC response to the 10 year old biofidelity targets.

1. Scale Normalized Adult PMHS Data to 10 Year Old Size

Dynamic thoracic spine data was obtained by testing adult PMHS in both ISM and sled tests with vertebral fixation [29-30]. Upper thoracic spine kinematic data was collected from three different PMHS (subject 330, 423, and 521) at two speeds along with T6 restraining force to get a characteristic force-displacement behavior of the T1-T6 vertebral segment (Figure 1). Two repeat tests were done on PMHS 521 at each speed.

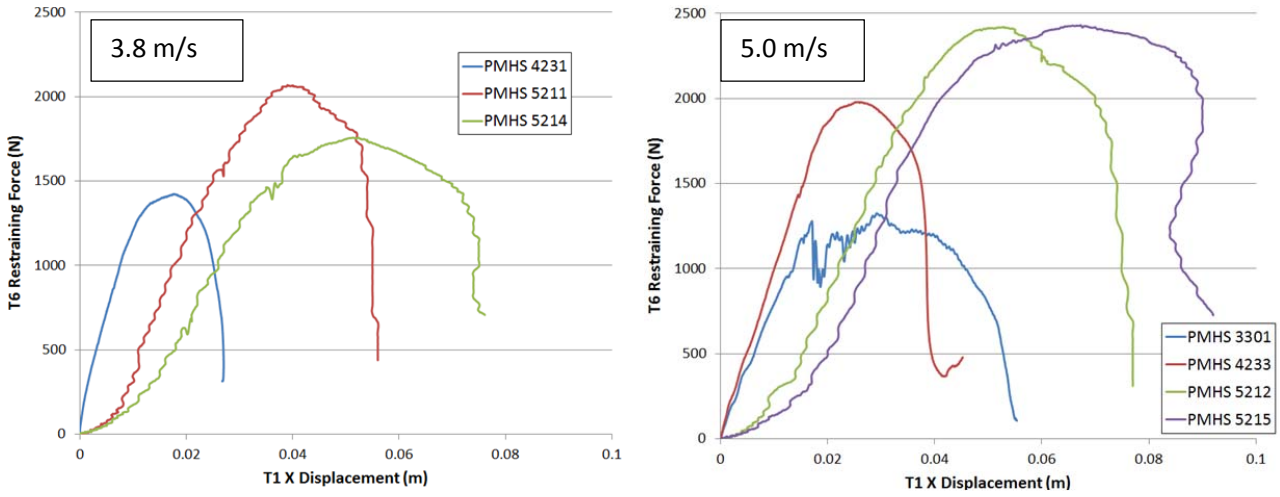

Figure 1. Adult PMHS thoracic spine data from Stammen et al [30].

This adult data was scaled so that the LODC upper torso response can be compared to the estimated response of a 10 year old child. Two methods from the literature were selected for scaling. Eppinger et al [25] introduced a mass scaling approach that assumed equal elastic modulus since scaling was done between adult subjects of different sizes. A length scale factor was calculated as the cube root of the ratio of the mass of the standard size subject to the actual subject, since equal density was assumed. Mertz et al [26] later adapted this method to derive response characteristics for a 10 year old by scaling the elastic modulus by age. This approach was applied to the three PMHS shown in Figure 1 (Table I).

TABLE I
SCALE FACTORS USING EPPINGER/MERTZ METHOD

Subject	λ_V	λ_{ME}	λ_E	λ_L	$\lambda_K = \lambda_E \lambda_L$	$\lambda_t = \lambda_E^{-1/2} \lambda_{ME}^{1/3}$	$R_F = \lambda_V \sqrt{\lambda_{ME}\lambda_K}$	$R_D = \lambda_V \sqrt{\lambda_{ME}/\lambda_K}$
PMHS 1 (330)	1	0.685	0.854	0.884	0.755	0.954	0.719	0.953
PMHS 2 (423)	1	0.638	0.854	0.815	0.696	0.932	0.667	0.957
PMHS 3 (521)	1	0.507	0.854	0.770	0.657	0.863	0.577	0.878

where λ_V is the impact velocity scale factor (PMHS and LODC are tested at the same speed), λ_{ME} is the subject mass scale factor (ratio of LODC mass to PMHS mass), λ_E is the elastic modulus scale factor reported for a 10 year old [26], λ_L is the ratio of LODC to PMHS height, λ_K is the stiffness scale factor (product of elastic modulus and length ratios), and λ_t is the time scale factor. The estimated 10 year old data was calculated by multiplying the adult PMHS force, displacement, and time data shown in Figure 1 by R_F , R_D , and λ_t respectively.

The second approach is a more recent method presented by Lopez-Valdes et al [28]. This method uses a work-energy balance to scale between adult and child force-displacement data from testing conducted in the same conditions. It assumes that the kinetic energy of the sled buck equals the work done by the seat belt restraining the forward motion of the occupant. The displacement and force scale factors are calculated by using peak belt force and subject mass measured in low speed sled tests conducted on both adult and pediatric volunteers [27]:

$$s_{ped} = \frac{m_{ped}}{m_{adult}} \frac{F_{adult(peak)}}{F_{ped(peak)}} s_{adult}$$

where the force and displacement scale factors are

$$R_F = \frac{F_{ped(peak)}}{F_{adult(peak)}}$$

$$R_D = \frac{s_{ped}}{s_{adult}} = \frac{m_{ped}}{R_F\, m_{adult}}$$

Using the average of the lap and shoulder belt peak forces and average subject masses from the 9-11 year old pediatric volunteers and adult volunteers reported in Arbogast et al [27] as shown in the Appendix, the force, displacement, and time scale factors are as follows:

$$R_F = \frac{337\ \text{N}}{668\ \text{N}} = 0.504$$

$$R_D = \frac{32.3\ \text{kg}}{(0.504)(80.2\ \text{kg})} = 0.799$$

$$\lambda_t = \lambda_E^{-1/2} \lambda_{ME}^{1/3} = (0.854)^{-1/2}(32.3/80.2)^{1/3} = 0.799$$

The adult PMHS data shown in Figure 1 was multiplied by these factors to generate a second estimated 10 year old dataset. Both this dataset and the Mertz-scaled dataset were used to develop ATD response targets.

2. Normalize the Scaled 10 Year Old Thoracic Spine Data

To derive biofidelity targets for the LODC, the two sets of scaled 10 year old data derived from the adult PMHS data were normalized separately using a deformation energy approach described in Donnelly et al. [31]. This technique builds on a previous technique by Moorhouse et al [32] and uses the energy under individual test force vs. displacement curves to normalize to a characteristic response. Biofidelity targets were then created for the normalized datasets from the two scaling methods using a two-dimensional ellipse approach [33].

3. LODC tests in ISM and Fixed Spine Biofidelity Conditions

The LODC thorax contains a flexible thoracic spine, softer and more anthropometrically accurate ribcage, multi-point thoracic deflection measurement, and humanlike shoulder construction developed and constructed to reflect recent pediatric biomechanical data. This thorax is intended for possible integration into the existing Hybrid III ten year old ATD to address artificially high head accelerations associated with chin-chest contact [7-8]. Figure 2 shows the LODC thorax in detail.

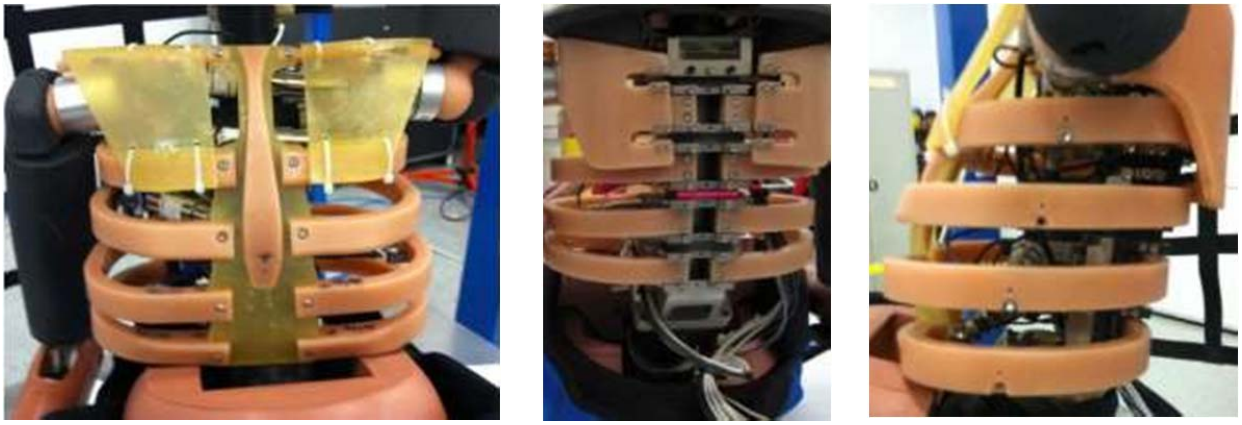

Figure 2. The Large Omnidirectional Child ATD Thorax (front, rear, and side views)

The biofidelity of the LODC thoracic spine was evaluated in two conditions used previously for adult PMHS thoracic spine evaluation: Isolated Segment Manipulation (ISM) and fixed spine sled [29-30]. Figure 3 shows the LODC setup for the ISM condition, where the head and neck are coupled together above the T1 location. This head-neck assembly is connected rigidly to the follower, which rides on the TAPPER cam mechanism. The displacement is measured by a 3aω motion block (3 accelerometers and 3 angular rate sensors mounted on a rigid cube) connected to the coupling plate. The force for each perturbation is measured by the HdT1 load cell. The T6 location of the LODC is rigidly fixed to the frame, with reaction loads measured by the T6 load cell. Figure 4 describes what happens in a single perturbation. A series of perturbations were obtained at 0.5 m/s linear velocity over a duration of 5 seconds, with no fixation at the pectoral girdle (PG) locations anterior to the thorax. An impulse response function (IRF) was calculated from the force and displacement data obtained over the duration. The IRF was then fit with a parametric model to obtain mechanical properties of the assumed second order system. The properties of the LODC were compared directly to the adult PMHS properties from Stammen et al [30].

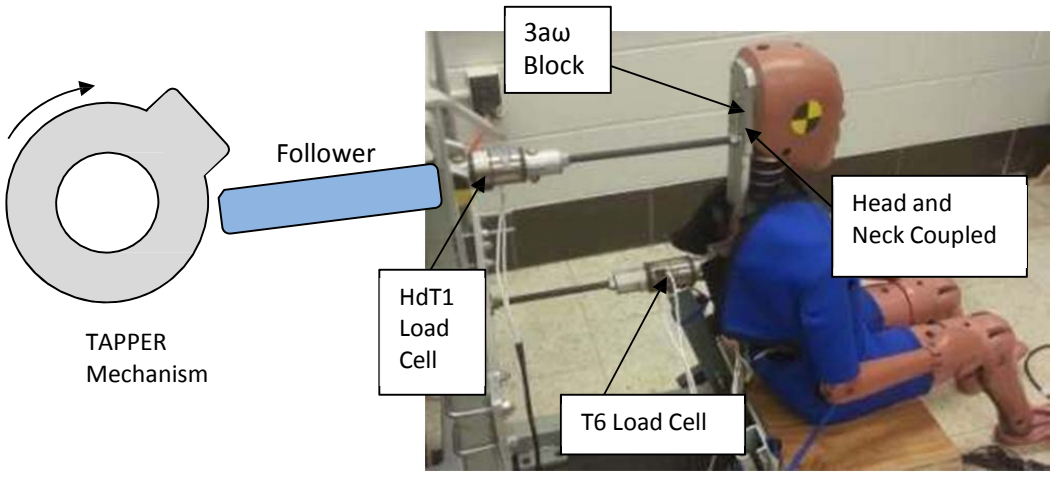

Figure 3. ISM test setup with LODC

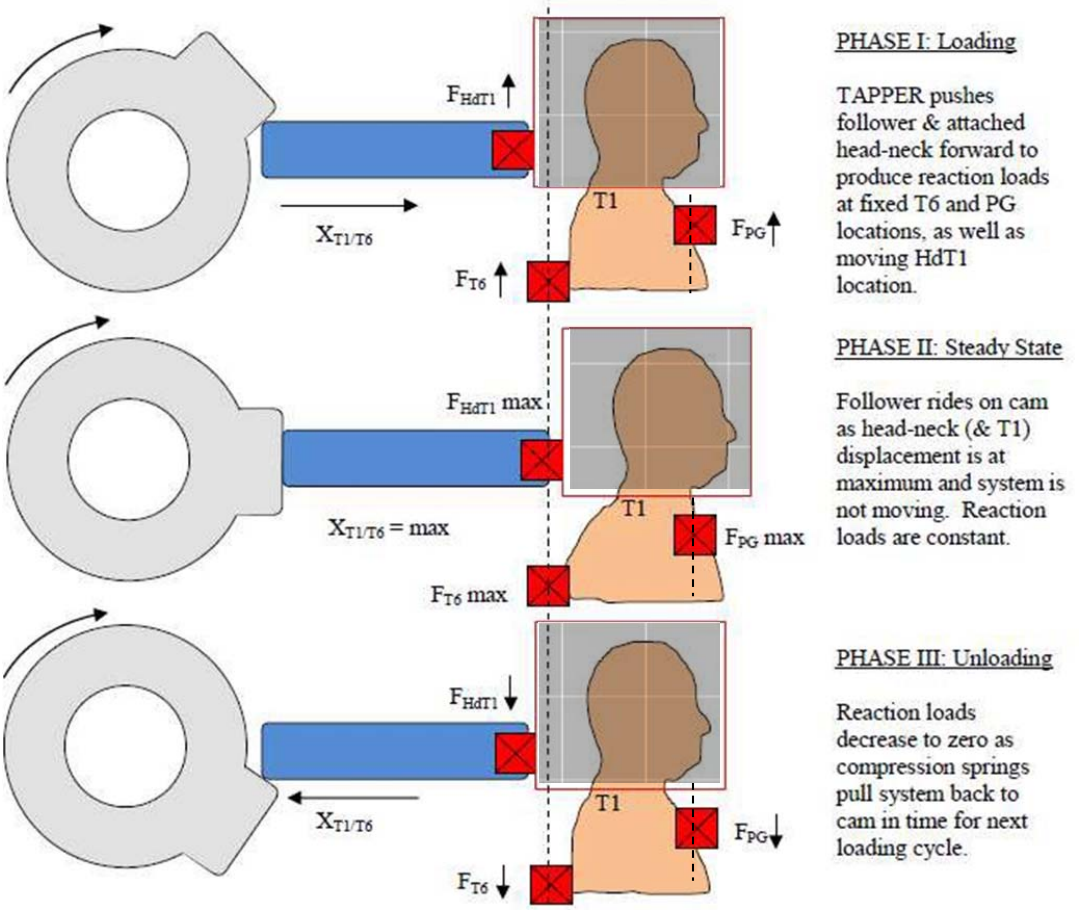

Figure 4. ISM loading phases for single perturbation (PG was not restricted in this test condition, $F_{PG} = 0$)

In the fixed spine sled condition (Figure 5), the mid spine (T6-T8) is rigidly coupled to the sled via a load cell to track the reaction loads while the thoracic spine kinematics are measured. The thoracic spine was instrumented at T1 and T6 with 3aω motion blocks (three accelerometers and three angular rate sensors) as shown in Figure 6. Three repeat tests were conducted at both 3.8 m/s and 5.0 m/s (pulses shown in Figure 7). The sled pulses were tuned to obtain T1/T6 relative velocities consistent with those reported in belted PMHS tests from the literature [34].

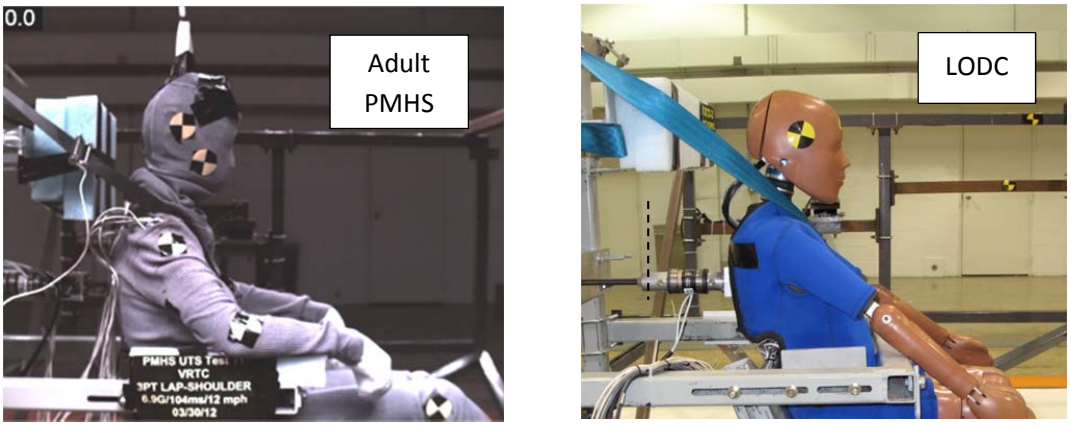

Figure 5. LODC in same vertebral fixation sled setup used to evaluate adult PMHS

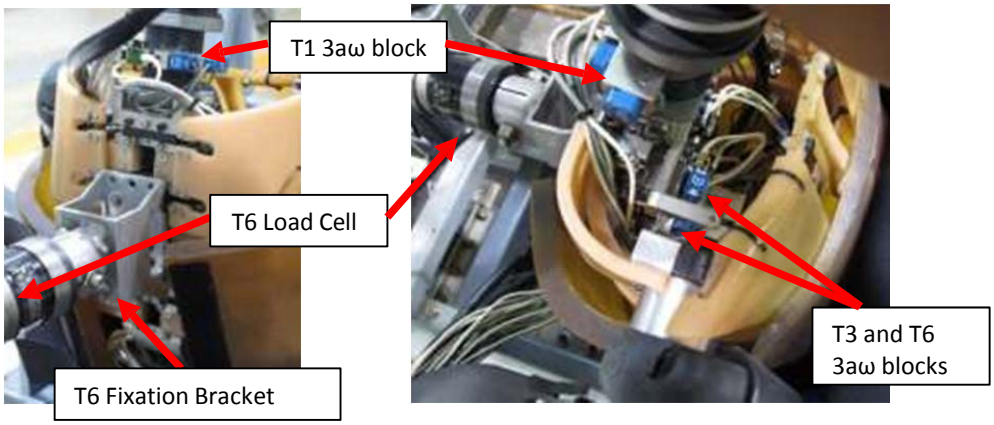

Figure 6. T6 attachment and kinematic instrumentation on LODC spine

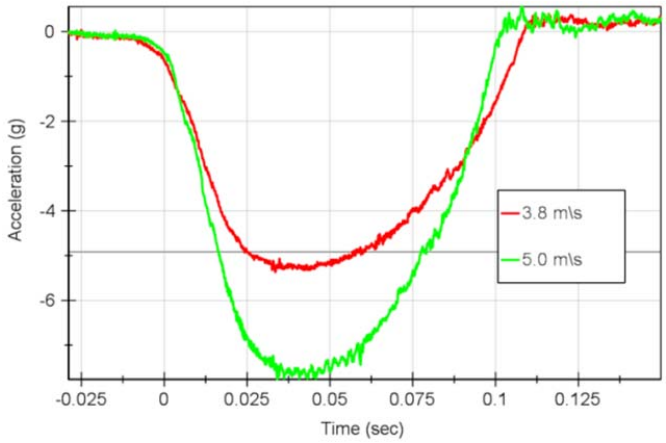

Figure 7. LODC sled pulses

4. Compare LODC to Biofidelity Targets

A parametric model was used to estimate mechanical properties of both the LODC and adult PMHS in the ISM tests. A parametric model of a second order damped system (Figure 8) was fit to the impulse response function to find the effective mass, stiffness, and damping coefficient of the T1-T6 segment [29].

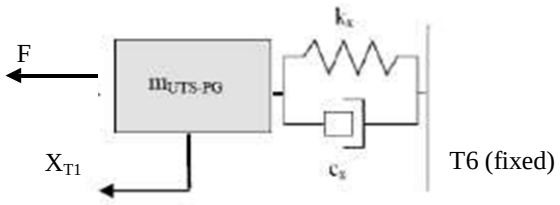

Figure 8. System model of T1-T6 body segment

In addition to comparing the mechanical properties of the LODC to the PMHS in the ISM condition, the biofidelity of the LODC thoracic spine response was quantified with respect to the scaled human data in the sled tests using the NHTSA Biofidelity Ranking System (BRS) [35]. Qualitative biofidelity assessment of LODC head motion was also conducted by applying a 1.7 scale factor (9-11 year old average = 38.6 deg, adult average = 22.8 deg) to head rotations as reported in [27]. The X and Z displacements were both scaled by a 0.799 scale factor using the method reported in [28]. To evaluate repeatability, percent coefficient of variation (%CV) was calculated for the peak displacement and force values in the three LODC tests at each speed, and average coefficient of variation was calculated over the full time history using the approach detailed in Moorhouse et al [32].

III. RESULTS

Figure 9 shows the IRF determined for the LODC test at 0.5 m/s perturbation velocity, along with the overlaid parametric model fit of the IRF to obtain effective mass, damping, and stiffness. Figures 10-12 show the LODC mean responses compared to both the Mertz and Lopez-Valdes scaled/normalized large child biofidelity targets. The LODC was tested three times at both speeds to evaluate repeatability. Table II compares the mechanical properties of the LODC directly to the adult PMHS properties in the ISM condition, which come from the second order system parametric model fit to the impulse response function (red dashed curve in Figure 9). Table III summarizes the BRS scores for each of the time history comparisons. Table IV summarizes the repeatability of the LODC force and displacement responses.

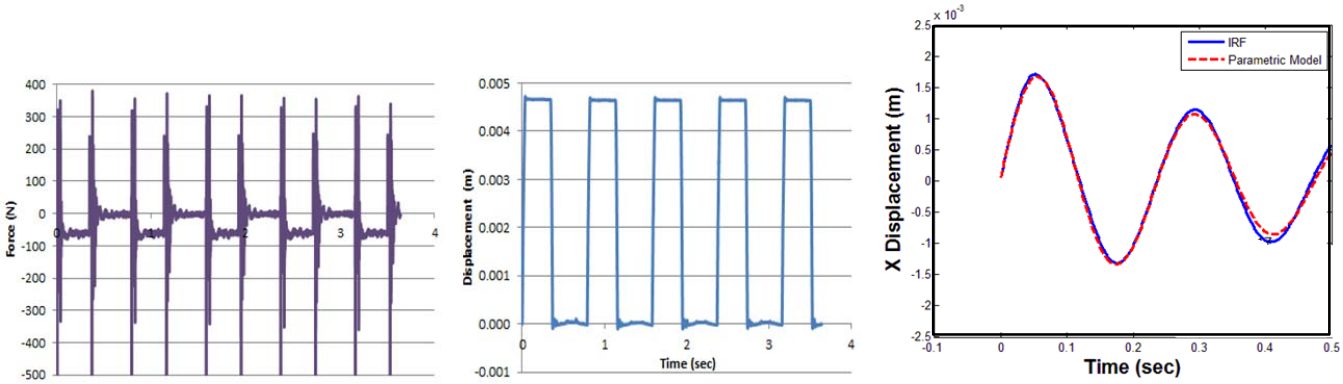

Figure 9. Force and displacement time histories & IRF parametric fit for LODC ISM test conducted at 0.5 m/s perturbation velocity

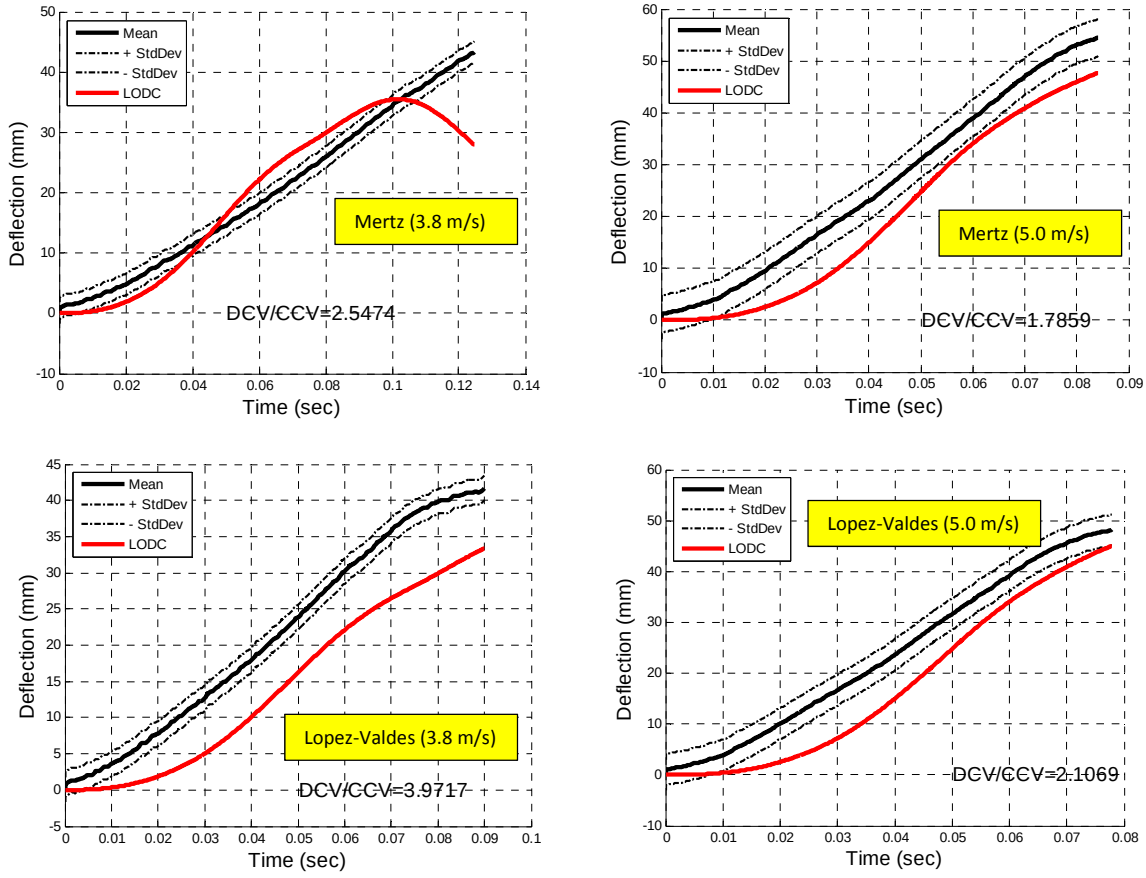

Figure 10. LODC mean displacement vs. time response compared with scaled/normalized biofidelity targets

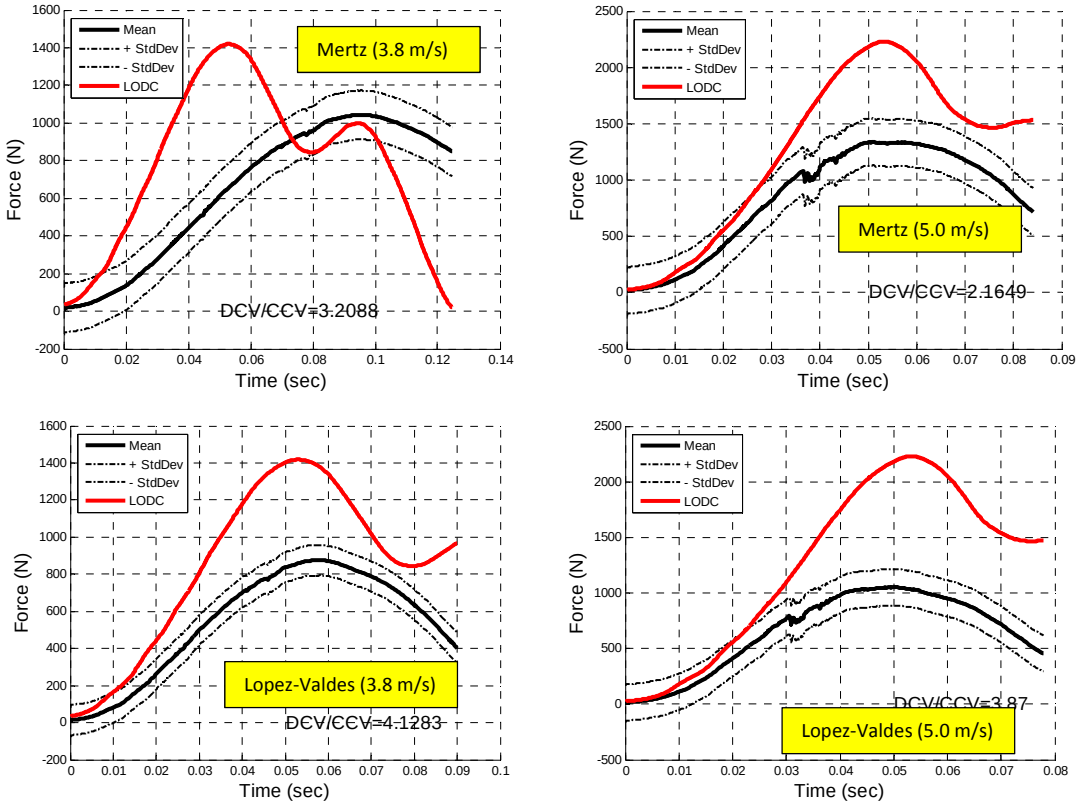

Figure 11. LODC mean force vs. time response compared with scaled/normalized biofidelity targets

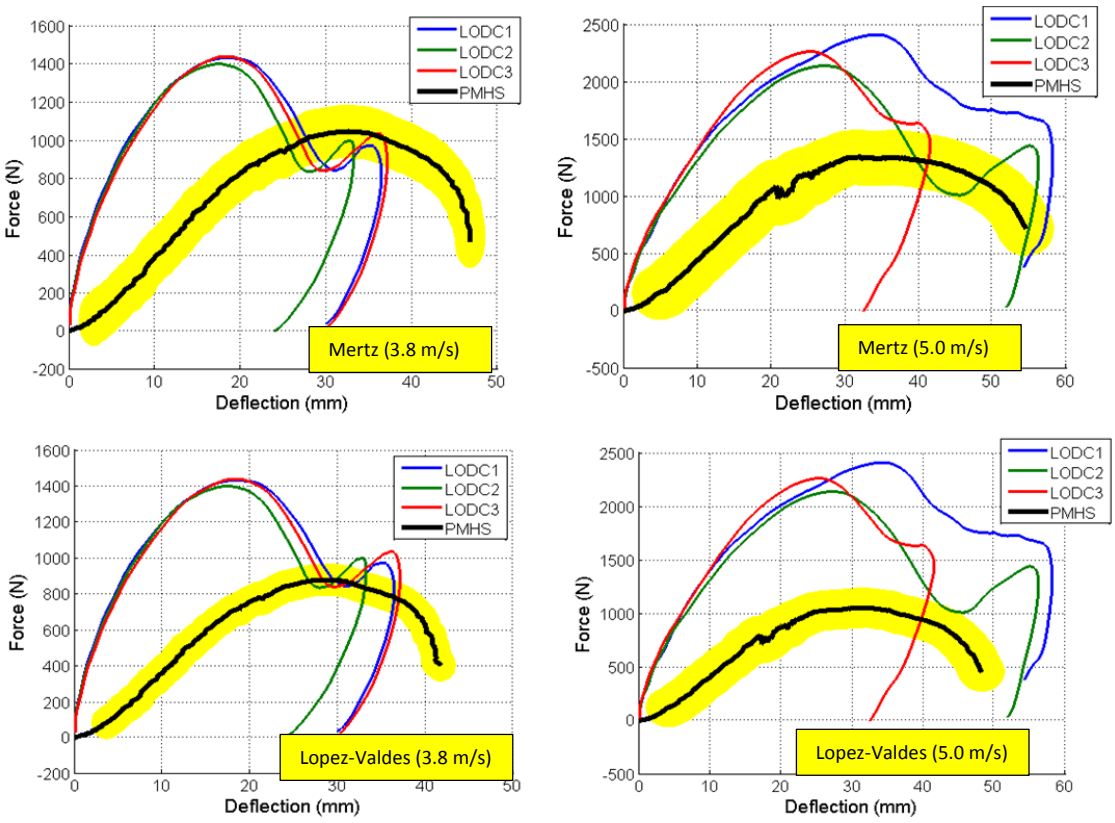

Figure 12. LODC force vs. displacement responses compared with scaled/normalized biofidelity targets

TABLE II
MECHANICAL PROPERTIES FROM ISM PARAMETRIC MODEL FITS

Subject	Test Condition	Speed[1] (m/s)	Effective Mass (kg)	Damping Coefficient (N-s/m)	Stiffness (kN/m)
Adult PMHS [2]	ISM	0.5	43.4	188	19.5
LODC	ISM	0.5	20.4	76	14.3

[1]ISM perturbation velocity representing relative speed of T1 with respect to T6; sled velocity is T6 velocity with respect to ground
[2]Average from same PMHS as used for the 3.8 and 5.0 m/s sled tests (Figure 1 and Table I). Data from [30].

TABLE III
LODC BIOFIDELITY RANKING SYSTEM SUMMARY

	Mertz		Lopez-Valdes	
	Displacement	Force	Displacement	Force
3.8 m/s	2.55	3.21	3.97	4.13
5.0 m/s	1.79	2.16	2.73	3.87

*A BRS score of 2 or lower is generally considered to be acceptable biofidelity.

TABLE IV
LODC REPEATABILITY ANALYSIS

Velocity	Measurement	n	Peak Values			Time History Average CV
			Mean	Standard Deviation	CV	
3.8 m/s	**T6 Force (N)**	3	1419	21.4	1.5%	4.7%
	T1 X Displacement (mm)		35.6	2.0	5.6%	5.5%
5.0 m/s	**T6 Force (N)**	3	2262	136.0	6.0%	12.6%
	T1 X Displacement (mm)		51.6	9.0	17.4%	15.0%

Figure 13 compares the LODC kinematically with adult PMHS in the 5.0 m/s sled condition.

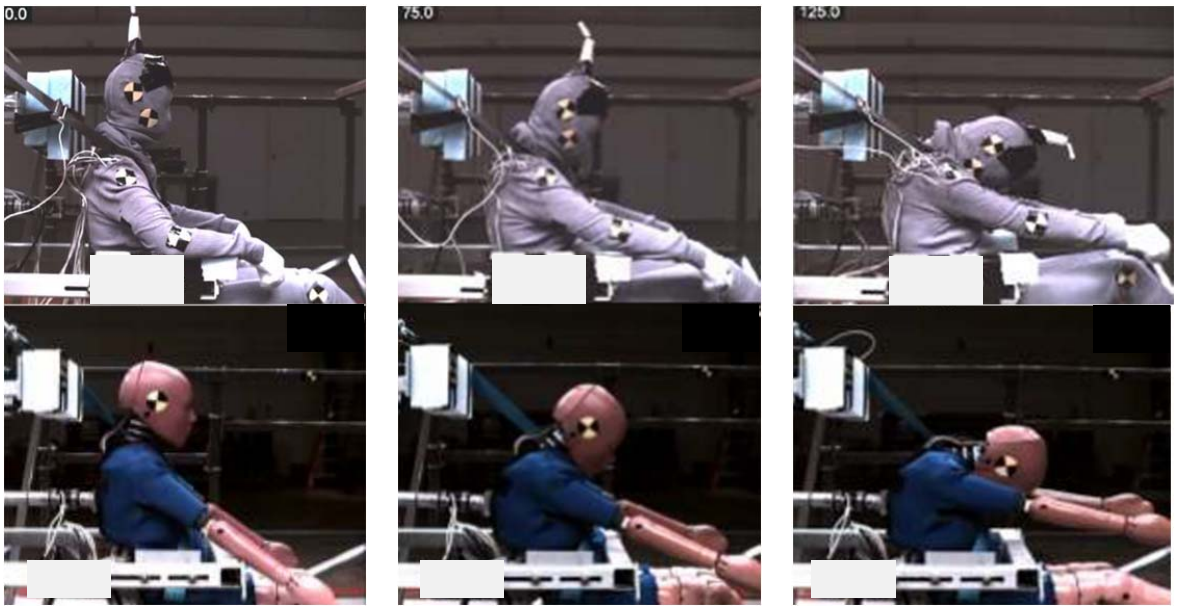

Figure 13. Adult PMHS vs. LODC screen captures to compare kinematics (5.0 m/s)

Figure 14 compares the LODC head rotations and trajectories to scaled adult PMHS data.

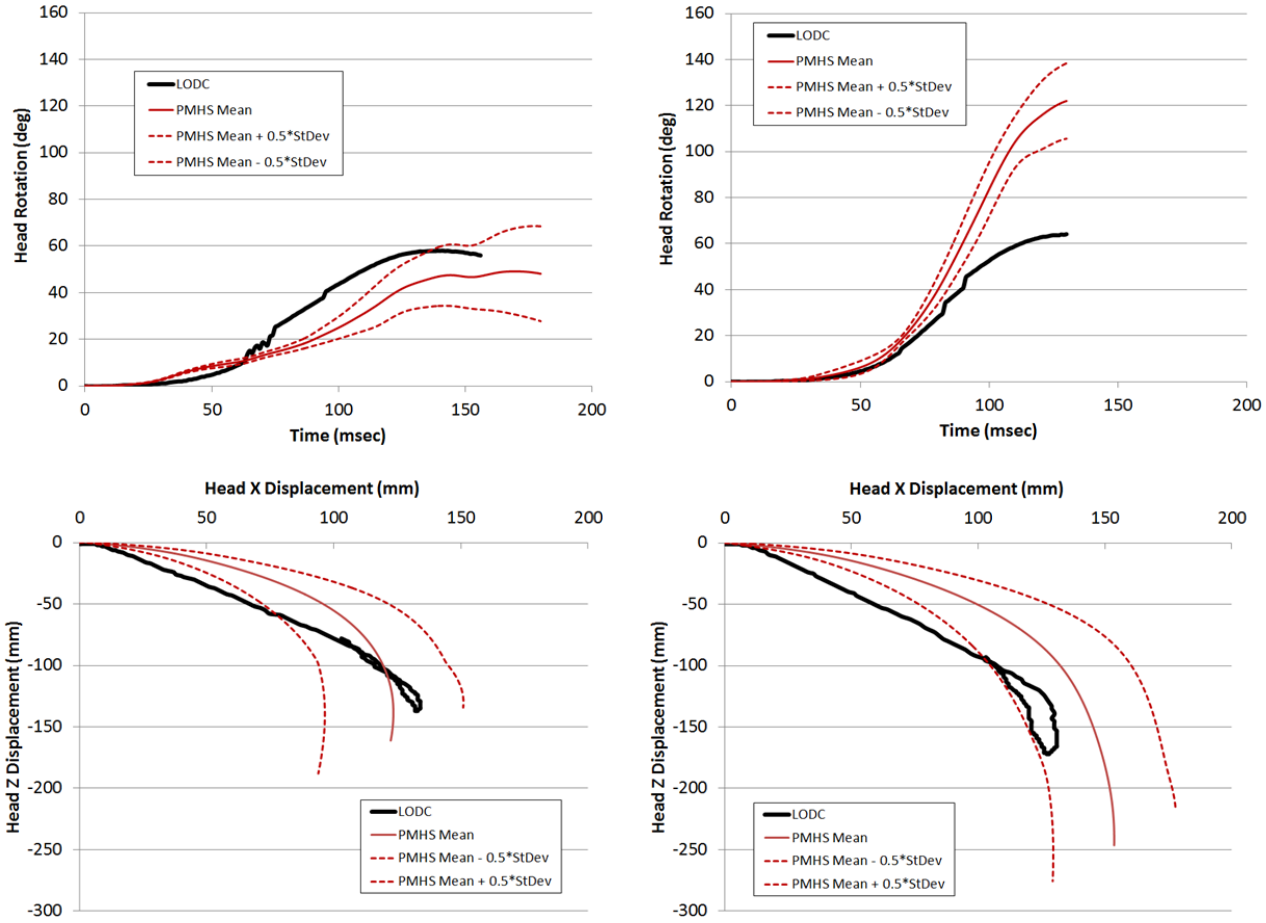

Figure 14. LODC vs. scaled adult PMHS head kinematics (left = 3.8 m/s, right = 5.0 m/s)

IV. DISCUSSION

In this study, adult PMHS thoracic spine data was scaled to estimated 10 year old targets in order to evaluate the biofidelity of a new large omnidirectional child (LODC) ATD thorax. The adult data was first scaled using two published techniques at two different speeds. The scaled responses were then normalized using a deformation energy technique to generate characteristic 10 year old target responses for biofidelity evaluation. Finally, the LODC was tested in the same conditions as the adult PMHS to evaluate its similarity to the human response targets.

To provide a direct comparison for LODC thoracic spine response, two published scaling approaches were applied to the adult PMHS data. The scale factors calculated using each method both reduced the displacement and force. The Mertz approach resulted in higher scale factors (R_F average = 0.654, R_D average = 0.929) than the Lopez-Valdes approach (R_F = 0.504, R_D = 0.799). Mertz scale factors were applied individually to each of the three PMHS, while the same scale factor was applied to all three PMHS using the Lopez-Valdes approach. The reason for this difference is that the factors from the Lopez-Valdes energy method were based on a pre-existing set of data from adult and child volunteers in the same condition, while the Mertz factors were dependent upon PMHS subject size and a published elastic modulus scale factor. The time scale factor for each target used the same equation and elastic modulus scale factor, with the difference being the mass scale factor. The Mertz time scale factor (average = 0.916) used the ratio of the LODC mass to individual adult PMHS mass, while the Lopez-Valdes time factor (0.799) used the ratio of the 9-11 year old pediatric volunteer mass average to the adult mass average. These differences

in scale factors applied to the adult PMHS had a relatively small influence on the target corridors generated after normalization (Figures 10-12). Given that the scale factors from either methodology have not been validated directly by human pediatric data at crash-level speeds, both approaches were applied and this comparison represents the best possible assessment of LODC thoracic spine biofidelity.

In comparing the LODC force vs. displacement response to the estimated human target response, the LODC peak forces were higher and peak displacements were lower than both the human targets at each speed. The LODC appears to be too stiff. The LODC showed a bi-modal response shape with a drop and then increase in force late in the event as opposed to a more uni-modal response displayed by the human (see Figure 12). It appears that the inertial component of the LODC response should be reduced somewhat in order to shift the peak force to a higher displacement level. Video analysis (Figure 13) showed very little cervical (neck) flexion in the LODC, and this is thought to be a function of a very soft cervicothoracic joint acting as a pivot in the LODC. This behavior indicates the need to design a smoother/gradual transition between the cervical and thoracic spine components.

To quantify the current biofidelity of the LODC thoracic spine, the BRS method was applied to the force and displacement time history data (Table III). BRS scores ranged from 1.79 for high speed displacement vs. the Mertz target to 4.13 for low speed force vs. the Lopez-Valdes based target. Typically, a score of 2 or less indicates that the next ATD test will be as close to the human mean response as the next human test [34]. The average BRS score was 3.05 ± 0.88, primarily because the forces were higher and displacements lower than the scaled PMHS data. However, note that the scaled human responses are only estimates, which also factors into the scores. Without scaling, the LODC scores would be better because of a closer match directly to adult PMHS response. While it is not generally acceptable to compare a child ATD response to adult human response, this similarity with human data demonstrates that the LODC spine has some biofidelic characteristics.

The primary motivation for a biofidelic child ATD thoracic spine is improved head kinematics. Figure 14 shows that both the LODC head rotation and trajectory fall within the estimated human response targets at 3.8 m/s, but the ATD head appears to fall short of both the rotation and trajectory targets at 5.0 m/s. It was observed that before scaling by the 1.7 factor derived from low speed volunteer testing, the LODC head rotation time history closely matched the unscaled adult PMHS head rotation at 5.0 m/s. Note that only one half standard deviation was used for the target bounds for both rotation and trajectory at each speed, which is less than the tolerance typically used in ATD corridors. Given that over-estimated head rotations and under-estimated head excursions have been reported for current child ATDs, it is encouraging that the LODC head appears to approximate human rotation and trajectory.

The ISM test condition provides another opportunity for comparing the LODC to human upper torso data. While this condition only evaluates response in the linear range, it does provide a direct dynamic comparison that captures a small window of motion consistent with the sled condition. Additionally, the ISM and sled tests were conducted on the same PMHS set so that the behavior in each test configuration can be compared for the same PMHS specimen. Table II shows that the effective stiffness of the LODC (K=14.3 kN/m) was 73.3% of that of the average from the three PMHS (K=19.5 kN/m). This percentage is similar to the stiffness scale factor (70.3%) noted in Table I. If the LODC accurately represents a 10 year old child in the ISM condition, this consistency in effective stiffness may imply that the Mertz scaling method is appropriate for estimating human response differences for different size/age specimens in the elastic range and that the elastic modulus scale factor is appropriate.

Repeatability is a concern when an ATD component is made more flexible. Table IV shows that the LODC was repeatable at 3.8 m/s but less repeatable at 5.0 m/s. This degradation in repeatability appears to be due to an increasing level of laxity discovered during inspection of the thoracic spine prior to the third 5.0 m/s test. In a subsequent test conducted at 5.8 m/s, there was a lateral delamination at the rubber-metal interface in the vertebral joint just above the fixation point at T6. While this durability issue was documented as a point of focus in future LODC testing, it should be noted that this unique spine fixation setup created a boundary condition with high stress concentration not normally present in a non-fixed scenario (such as a child restraint test). If this setup is used to evaluate future LODC design iterations, a more distributed fixation will be required especially if testing is conducted at higher sled speeds.

The relative velocity of T1 versus T6 in the ISM test is 0.5 m/s, which is somewhere between the T1/T6 spine velocities measured in the 3.8 m/s and 5.0 m/s sled tests. This range of sled velocity was used because it was expected to produce T1/T6 relative spine velocities similar to three-point belted PMHS sled tests at 40 km/h from

Shaw et al. [34] using the ISM-derived PMHS mechanical properties [30]. The lower effective mass and lower damping coefficient for LODC than the PMHS (see Table II) may be due to less viscous elements within the thorax and abdomen than in the PMHS. While there is undoubtedly relative motion between internal organs and the thorax in the PMHS, there is no such phenomenon occurring within the LODC thorax and abdomen to influence the inertial/viscous response.

A limitation of this study is that the focus was solely on X displacement/forces rather than rotation/moment or Z tension/compression because there was very little rotation of T1 relative to T6 observed in PMHS sled testing. Nearly all the rotation was in the head and cervical spine. Additionally, to calculate the mechanical properties in the ISM condition, the spine was modeled as a one-dimensional system. To more comprehensively model the complex spine dynamics, a model incorporating both translational and rotational characteristics could provide a better comparison of mechanical properties for the ATD vs. human data. Another limitation is that only three PMHS were available for the creation of biofidelity targets.

In summary, this study provides an initial assessment of LODC thoracic spine biofidelity. Similarities and differences between the LODC and scaled human targets were identified, and this evaluation will help to guide design improvements for the next version of the LODC. The LODC appears to possess characteristics that result in dynamic behavior that is approximating human response in both spine force vs. displacement and head kinematics. Optimization of overall spinal curvature, with adjustments to the cervicothoracic joint and refinement of individual tunable vertebral elements, should result in a response more closely matching the biofidelity targets. Future work will focus on improving the biofidelity, repeatability, and durability of the LODC design and comparing it to the Hybrid III 10 year old and Q10 ATDs in both component and sled level evaluations.

V. CONCLUSIONS

- A prototype flexible thorax, referred to as the large omnidirectional child (LODC), has been developed to address uncertainties with head kinematics in current child ATDs.
- The biofidelity of the LODC flexible spine thorax was evaluated by comparing its response with scaled/normalized PMHS thoracic spine data in two test configurations (ISM and fixed spine sled).
- The LODC displayed some similar characteristics to estimated human large child response targets in both thoracic spine force vs. displacement and head kinematics. However, the LODC spine was stiffer than the estimated large child human targets, with BRS scores in the sled condition ranging from 1.79 – 4.13 across force-time and displacement-time at two speeds with two different scaled targets. As a result, the LODC head rotations and trajectories were somewhat lower than scaled adult PMHS head kinematics. The LODC-adult PMHS effective stiffness ratio in the ISM condition was consistent with the stiffness scale factor reported in the literature.
- The primary area of improvement was determined to be the cervicothoracic joint, where a low rotational stiffness resulted in a bi-modal response shape. Optimization of this area of the spine along with a softer thoracic spine is expected to change the overall shape of the response to be more consistent with the biofidelity targets.
- The repeatability of the spine response was good at 3.8 m/s but degraded at 5.0 m/s. This behavior will be monitored as the LODC design evolves.
- Future work will focus on improving the LODC design using the data from this initial evaluation and comparing the LODC with the Hybrid III 10 year old and Q10 ATDs in both component and sled level evaluations.

VI. ACKNOWLEDGEMENTS

The authors thank Children's Hospital of Philadelphia for providing their low speed volunteer data.

VII. REFERENCES

[1] Sherwood C, et al. "Prediction of Cervical Spine Injury Risk for the 6-Year-Old Child in Frontal Crashes," *AAAM*

(2002).
[2] Ash J, et al. "Comparison of Anthropomorphic Test Dummies with a Pediatric Cadaver Restrained by a Three-Point Belt in Frontal Sled Tests," Paper No. 09-0362, *Enhanced Safety of Vehicles* (2009).
[3] Seacrist T, et al. "Kinematic Comparison of Pediatric Human Volunteers and the Hybrid III 6-Year-Old Anthropomorphic Test Device," *AAAM* (2010).
[4] Seacrist T, et al. "Kinematic Comparison of the Hybrid III and Q-Series Pediatric ATDs to Pediatric Volunteers in Low-Speed Frontal Crashes," *AAAM* (2012).
[5] Seacrist T, et al. "Comparison of the Q-Series ATDs to Child Volunteers in Low-Speed Sled Tests," *Protection of Children in Cars* (2013).
[6] Wu J, et al. "A Simulation Study of Spine Biofidelity in the Hybrid-III 6-Year-Old ATD," *Traffic Inj Prev* (2013).
[7] Stammen J, et al. "Biomechanical Impact Response of the Human Chin and Manubrium," *Ann Biomed Eng* (2011).
[8] NHTSA Code of Federal Regulations, Federal Motor Vehicle Safety Standard No. 213: "Child Restraints" (2012).
[9] Arbogast et al. "Effectiveness of Belt Positioning Booster Seats: An Updated Assessment," *Pediatrics* (2009).
[10] Ching R, et al. "Tensile Mechanics of the Developing Cervical Spine," Paper 2001-22-0015, Forty-Fifth Stapp Car Crash Journal (2001).
[11] Luck J, et al. "Tensile Mechanical Properties of the Perinatal and Pediatric PMHS Osteoligamentous Cervical Spine," Paper No. 2008-22-0005, *Fifty-Second Stapp Car Crash Journal* (2008).
[12] Nuckley D, et al. "Developmental Biomechanics of the Cervical Spine: Tension and Compression," *J Biomechanics* 39 (2006): 3045-3054.
[13] Barros E, et al. "Aging of the Elastic and Collagen Fibers in the Human Cervical Interspinous Ligaments," *The Spine Journal*, Vol. 2 (2002): 57-62.
[14] Bilston L, et al. "Pediatric Spinal Injury Type and Severity Are Age and Mechanism Dependent," *Spine* 32; 21 (2007).
[15] O'Gorman H, et al. "Thoracic Kyphosis and Mobility: The Effect of Age," *Physiotherapy Practice* (1987); 3: 154-162.
[16] Arbogast K, et al. "Normal Cervical Spine Range of Motion in Children 3–12 Years Old," *Spine* 32; 10 (2007).
[17] Greaves L, et al. "The Effect of Age and Gender on the Three-Dimensional Kinematics of the Pediatric Cervical Spine," *SAE* Paper No. 2007-01-2495 (2007).
[18] Willems J, et al. "An *In Vivo* Study of the Primary and Coupled Rotations of the Thoracic Spine," *Clinical Biomechanics* 11; 6 (1996).
[19] Kallieris D, et al. "Comparison between Child Cadavers and Child Dummy Using Child Restraint Systems in Simulated Collisions," Paper No. 760815, *Twentieth Stapp Car Crash Journal* (1976).
[20] Kallieris D, et al. "Response and Vulnerability of the Human Body at Different Impact Velocities in Simulated Three-Point Belted Cadaver Tests," *IRCOBI* (1978).
[21] Brun-Cassan F, et al. "Comparative Study of Restrained Child Dummies and Cadavers in Experimental Studies," Paper 933105, *Society of Automotive Engineers* (1993).
[22] Dejeammes M, et al. "Exploration of Biomechanical Data towards a Better Evaluation of Tolerance for Children Involved in Automotive Accidents," Paper 396 (1984).
[23] Wismans J, et al. "Child Restraint Evaluation by Experimental and Mathematical Simulation," Paper 791017, *Society of Automotive Engineers* (1979).
[24] Mattern R, et al. "Reanalysis of Two Child PMHS Tests," Final Report, University of Heidelberg, Heidelberg, Germany (2002).
[25] Eppinger R, et al. "Development of Dummy and Injury Index for NHTSA's Thoracic Side Impact Protection Research Program," SAE 840885 (1984).
[26] Mertz H, et al. "The Hybrid III 10 Year Old Dummy," *Stapp Car Crash Conference* (2001).
[27] Arbogast K, et al. "Comparison of Kinematic Responses of the Head and Spine for Children and Adults in Low-Speed Frontal Sled Tests," *Stapp Car Crash Journal* (2009).
[28] Lopez-Valdes F, et al. "Comparing the Kinematics of the Head and Spine between Volunteers and PMHS: a Methodology to Estimate the Kinematics of Pediatric Occupants in a Frontal Impact," *IRCOBI* (2011).

[29] Stammen J, et al. "Sequential Biomechanics of the Human Upper Thoracic Spine and Pectoral Girdle," *AAAM* (2012).
[30] Stammen J, et al. "Dynamic Properties of the Upper Thoracic Spine-Pectoral Girdle (UTS-PG) System and Corresponding Kinematics in PMHS Sled Tests," *Stapp Car Crash Conference* (2012).
[31] Donnelly B, et al. "A Deformation Energy Approach to Normalizing PMHS Response Data and Developing Biofidelity Targets for Dummy Design," Submitted to *IRCOBI* (2014).
[32] Moorhouse K, et al. "An Improved Normalization Methodology for Developing Mean Human Response Curves," *Enhanced Safety of Vehicles* (2013).
[33] Donnelly B, et al. "A Methodology for Creating PMHS Targets with a Two-Dimensional Standard Deviation Ellipse Tolerance for Quantitatively assessing Dummy Biofidelity," *IRCOBI* (2013).
[34] Shaw G, et al. "Impact Response of Restrained PMHS in Frontal Sled Tests: Skeletal Deformation Patterns Under Seat Belt Loading," *Stapp Car Crash Journal* (2009).
[35] Rhule H, et al. "A Methodology for Generating Objective Targets for Quantitatively Assessing the Biofidelity of Crash Test Dummies," *Enhanced Safety of Vehicles* (2013).

APPENDIX

TABLE A-1
PEDIATRIC VOLUNTEER DATA FROM ARBOGAST ET AL [2009]

Subject ID	Shld Belt Force (N)	Lap Belt Force (N)	Avg S-L Belt (N)	Mass (kg)
11	186	133	159	25
8	255	206	230	29
28	479	519	499	40
18	276	117	196	33
26	388	407	397	31
20	415	663	539	36
Average	**333**	**341**	**337**	**32.3**
Std Deviation	**111**	**224**	**163**	**5.3**

TABLE A-2
ADULT VOLUNTEER DATA FROM ARBOGAST ET AL [2009]

Subject ID	Shld Belt Force (N)	Lap Belt Force (N)	Avg S-L Belt (N)	Mass (kg)
37	801	662	731	74
33	811	527	669	84
34	691	368	530	97
36	860	601	730	65
21	805	700	753	65
23	776	597	687	87
24	779	360	570	107
35	713	364	539	68
22	756	666	711	74
27	872	652	762	81
Average	**786**	**550**	**668**	**80.2**
Std Deviation	**57**	**136**	**89**	**13.9**